

Petra S. Hüppi, M.D.

Department of Pediatrics, Children's Hospital, University Hospitals of Geneva, 6 rue Willy-Donze, 1211 Geneva 14, Switzerland

## Introduction

Understanding early human brain development is of great clinical importance, as many neurological and neurobehavioral disorders have their origin in early structural and functional brain development. With conventional magnetic resonance imaging we have been able to delineate macroscopically early developmental events such as myelination and gyral development. Diffusion tensor imaging (DTI) is a relatively new MR modality that assesses water diffusion in biological tissues at a microstructural level (1).

The developing human brain presents several challenges for the application of diffusion tensor imaging (DTI). Values for the water apparent diffusion coefficient and diffusion anisotropy differ markedly between pediatric brain and adult brain and vary with age. As a result, much of the knowledge regarding DTI derived from studies of mature, adult human brain is not directly applicable to developing brain. Yet in these challenges also lies opportunity, as changes in water apparent diffusion coefficient and diffusion anisotropy during development provide unique insight into the structural basis of brain maturation.

In addition to providing information on brain maturation, DTI may be used to evaluate brain injury. It is well known from studies of animals (3) and adult humans (4) that DTI can serve as an early indicator of stroke, often demonstrating image abnormalities on water diffusion maps well before conventional MRI. Early detection of injury is particularly critical in the context of administration of neuroprotective therapies to infants. These therapies must typically be initiated quickly – within hours of onset of injury – in order to interrupt the cascade of irreversible brain injury. Because these interventions are in themselves not without risk to the developing brain, it is of utmost importance to develop imaging tools that can reliably identify ongoing brain injury early to prevent treatment of non-injured patients (5). Water diffusion maps derived from DTI may provide the means for this early detection of injury. Changes in diffusion characteristics further provide early evidence of both focal and diffuse brain injury in association with periventricular leukomalacia (PVL), the most common form of white matter injury in the preterm infant (6). Finally with the development of 3D diffusion tensor fiber tractography maturation of white matter and its consequences for white matter connectivity can be followed throughout infant development into adulthood with the potential to study correlations between abnormalities on DTI and ultimate neurologic/cognitive outcome (7).

In the course, we will discuss the changes in DTI parameters associated with normal brain maturation as well as their response to brain injury. It is worth noting that the precise DTI parameters to employ is open to question. Diffusion parameters describing the brain's microstructure include the three diffusion eigenvalues ( $\lambda_1$ ,  $\lambda_2$ ,  $\lambda_3$ ), the apparent diffusion coefficient and a mathematical measure of anisotropy. There is a general consensus that the

directionally-averaged, rotationally-invariant water diffusion coefficient (the average apparent diffusion coefficient, or  $D_{av}$ ) is a useful parameter to derive from the diffusion tensor and serves as an indicator of brain maturation and/or injury.  $D_{av}$  is calculated as one third of the trace of the diffusion tensor, and provides the overall magnitude of water diffusion independent of anisotropy(8). In contrast, the descriptions of water diffusion anisotropy used by different research groups varies (*e.g.*, lattice anisotropy index, relative anisotropy, fractional anisotropy,  $A_{\varphi}$ , color directional plots of anisotropy, «vector maps» or «whisker plots,» gamma variate anisotropy images). These different representations of anisotropy are related to one another; their mathematical interconversions ranging from multiplication by a simple constant to complete recalculation using the underlying eigenvectors (9) in which the primary eigenvector describes the diffusivity parallel to axonal bundles, while the second and third eigenvector describes diffusivity orthogonal to the axonal bundles. Further, the optimal means by which to display water diffusion anisotropy remains an area of active investigation (10). Relative anisotropy (RA) or fractional anisotropy (FA) is an indicator of the degree of water diffusion anisotropy independent of the overall water diffusion coefficient. RA is zero for isotropic diffusion (diffusion that is equal in all directions) and approaches 1 as anisotropy increases. Notably, RA is linear over the total range of anisotropy values (9) for which there is some indication that the term FA represents changes in very low anisotropy such as found in the immature brain better than RA (10). Vector maps, which are typically overlaid on structural images, indicate the orientation of the major eigenvector of the diffusion tensor. They provide an indication of the direction in which water diffusion is highest, which typically is parallel to white matter tracts. Fiber tracking uses each voxel's primary eigenvector of the diffusion tensor to follow an axonal tract in 3D from voxel to voxel through the brain, thus allowing to delineate specific cerebral white matter connectivity. All three parameters are orientation-independent, meaning that they are not affected by the position of the subject in the MR scanner magnet relative to the orientation of the magnetic field gradients used to measure the diffusion values.

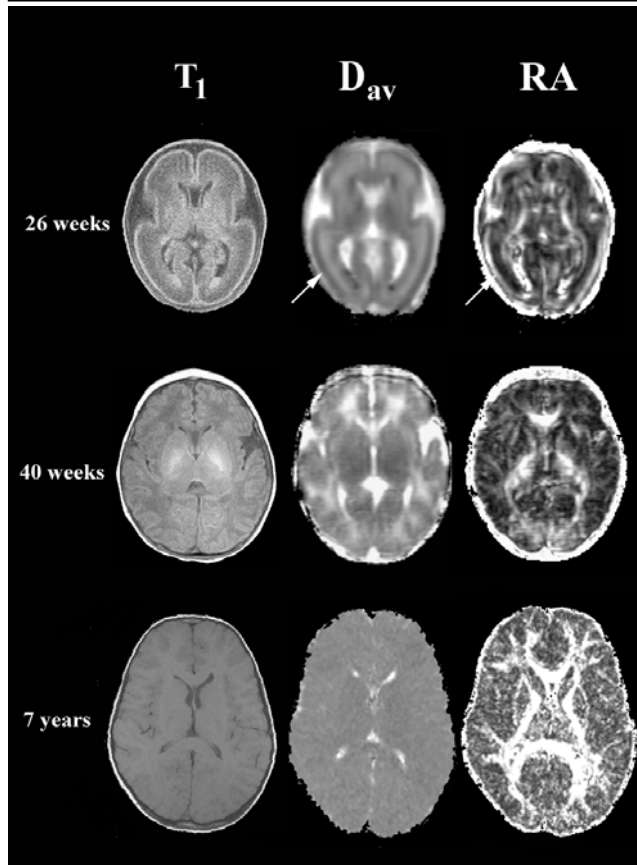
One aspect of DTI which differs between newborn infants and adults is the optimum  $b$  value at which to make the measurement. In general, a  $b$  value corresponding to approximately  $1.1/D_{av}$  provides the greatest contrast-to-noise ratio for such a measurement (11). In adult humans, the high  $b$  value is typically on the order of  $1000 \text{ mm}^2/\text{s}$ . For infant brain, which has higher values for  $D_{av}$ ,  $b$  values on the order of  $700\text{-}800 \text{ mm}^2/\text{s}$  are used. Otherwise, similar MR pulse sequences and post processing methods are used for both infant and adult human brain DTI.

### **DTI in Normal Brain Development**

$D_{av}$  values differ between pediatric and adult human brain in two primary ways. First,  $D_{av}$  values are higher for pediatric brain than adult. For example,  $D_{av}$  values for the white matter of the centrum semiovale in premature infants (12, 13) approach  $2.0 \times 10^{-3} \text{ mm}^2/\text{s}$ , while values for adult brain are typically  $0.7 \times 10^{-3} \text{ mm}^2/\text{s}$ .  $D_{av}$  values decrease with increasing age in a monotonic fashion during development until they reach adult values (14, 15). Second,  $D_{av}$  maps of pediatric brain show contrast between white and grey matter, with the  $D_{av}$  values for white matter being higher than those for grey matter (see Figure 1)

The center column consists of  $D_{av}$  parametric

Figure 1 Axial images at the level of the basal ganglia from subjects of differing ages (2)



maps for which higher values of  $D_{av}$  appear brighter. The right column consists of relative anisotropy (RA) parametric maps for which higher values of RA appear brighter. These changes are not necessarily simultaneous in all brain regions. Partridge S et al (16) defined white matter tract maturation in commissural tracts, such as the corpus callosum, in projection tracts such as the corticospinal tracts both inside the internal capsule as well as in the centrum semiovale and in association tracts such as the cingulum or the inferior longitudinal fasciculus using a high resolution DTI sequence. The lowest values of  $D_{av}$  was found in the projection fibers of the internal capsule and the cerebral peduncles with decreasing values from 30 to weeks gestational age to term age (normal gestation newborn). The greatest decrease in  $D_{av}$  over the observed time period occurred in the lower centrum semiovale (16). The precise cause of the decrease in  $D_{av}$  with increasing age is not known, though it has been postulated that the rapid decrease observed between early gestation and term is due to the concomitant decrease in overall water content (13). For reference, the  $D_{av}$  of free water at body temperature is approximately  $3.0 \times 10^{-3} \text{ mm}^2/\text{s}$ . Thus, there is some restriction to water motion even for the highest  $D_{av}$  values measured in premature infants, which are on the order of  $2.0 \times 10^{-3} \text{ mm}^2/\text{s}$ . Brain water content decreases dramatically with increasing gestational age. As it does, structures that hinder water motion (*e.g.*, cell and axonal membranes) become more densely packed, increasing restriction to motion; as if the brain becomes more viscous as its water content decreases. That not all of these changes in  $D_{av}$  are due to reduction in overall water content is confirmed by measurements of the three eigenvalues  $\lambda_1, \lambda_2, \lambda_3$ , which represent diffusion along the three major principal axes. During **white matter** development changes in diffusion (decrease) are observed primarily in  $\lambda_2, \lambda_3$  and not in  $\lambda_1$ , which reflect changes in

maps for which higher values of  $D_{av}$  appear brighter. The right column consists of relative anisotropy (RA) parametric maps for which higher values of RA appear brighter. These changes are not necessarily simultaneous in all brain regions. Partridge S et al (16) defined white matter tract maturation in commissural tracts, such as the corpus callosum, in projection tracts such as the corticospinal tracts both inside the internal capsule as well as in the centrum semiovale and in association tracts such as the cingulum or the inferior longitudinal fasciculus using a high resolution DTI sequence. The lowest values of  $D_{av}$  was found in the projection fibers of the internal capsule and the cerebral peduncles with decreasing values from 30 to weeks gestational age to term age (normal gestation newborn). The greatest decrease in  $D_{av}$  over the observed time period occurred in the lower centrum semiovale (16). The precise cause of the decrease in  $D_{av}$  with increasing age is not known, though it has been postulated that the rapid decrease observed between early gestation and term is due to the concomitant decrease in overall water content (13). For reference, the  $D_{av}$  of free water at body temperature is approximately  $3.0 \times 10^{-3} \text{ mm}^2/\text{s}$ . Thus, there is some restriction to water motion even for the highest  $D_{av}$  values measured in premature infants, which are on the order of  $2.0 \times 10^{-3} \text{ mm}^2/\text{s}$ . Brain water content decreases dramatically with increasing gestational age. As it does, structures that hinder water motion (*e.g.*, cell and axonal membranes) become more densely packed, increasing restriction to motion; as if the brain becomes more viscous as its water content decreases. That not all of these changes in  $D_{av}$  are due to reduction in overall water content is confirmed by measurements of the three eigenvalues  $\lambda_1, \lambda_2, \lambda_3$ , which represent diffusion along the three major principal axes. During **white matter** development changes in diffusion (decrease) are observed primarily in  $\lambda_2, \lambda_3$  and not in  $\lambda_1$ , which reflect changes in

water diffusion perpendicular to white matter fibers and may indicate changes due to premyelination (change of axonal width) and myelination(14).

Differences in water content may also underlie the contrast present between white and grey matter in pediatric brain, though not in a simple fashion. In adult brain, the water content of white matter is substantially lower than that of grey matter (65% vs. 85%<sup>23</sup>), yet the  $D_{av}$  values for the two regions are virtually identical (17). This implies that white matter is less restrictive to water motion than grey matter at a given water content. This may be related to the fact that water motion parallel to axons is relatively unrestricted, especially in comparison to motion perpendicular to axons or in grey matter. In the premature brain, water content is similar in white and grey matter. The finding of higher  $D_{av}$  values in white matter than grey for premature brain despite their similar water content is also consistent with the idea that white matter is less restrictive to water motion than grey matter. In adult brain, this difference in restriction appears to be offset by the differing water contents of the two areas.

Anisotropy values also differ between adult and pediatric brain. For children beyond term and for adults, anisotropy values for cortical grey matter are consistent with zero, meaning that water diffusion in grey matter is isotropic at the spatial resolutions currently available. Anisotropy values for white matter areas, on the other hand, are relatively low in infants and increase steadily with increasing age(18). As with changes in values for  $D_{av}$ , changes in relative or fractional anisotropy take place more quickly early in development. While changes in  $D_{av}$  and anisotropy for white matter typically take place in tandem, with  $D_{av}$  values decreasing and anisotropy values increasing during maturation, it is important to bear in mind that the two parameters are theoretically independent of one another. Thus, a change in one is not always accompanied by the opposite change in the other. For example, the decrease of anisotropy of cerebral cortex that takes place between 26 and 32 weeks gestational age is accompanied by a decrease in  $D_{av}$ (2).

The increase in white matter anisotropy values during development appears to take place in two steps. The first increase takes place *before* the histologic appearance of myelin (12, 13). This increase has been attributed to changes in white matter structure which accompany the «premyelinating state» (19). This state is characterized by a number of histologic changes, including an increase in the number of microtubule-associated proteins in axons, a change in axon caliber, and a significant increase in the number of oligodendrocytes. It is also associated with changes in the axonal membrane, such as an increase in conduction velocity and changes in  $Na^+/K^+$ -ATPase activity. Interestingly the commissural fibers in the splenium and the genu of corpus callosum express the highest fractional anisotropy values in the immature human brain (16). These fibers are largely unmyelinated in the newborn period (20) and their high anisotropy is in part due to a high degree of parallel organization. The second, more sustained increase in anisotropy, is associated with the histologic appearance of myelin and its maturation. The increase in anisotropy associated with premyelination is notable in that it takes place in the absence of changes in T1- or T2-weighted imaging as well as before the histologic appearance of myelin. Thus, it constitutes the earliest indication of impending myelination. The earliest signs of this second stage change in anisotropy is observed in the projections fibers of the posterior limb of the internal capsule in the newborn period. This two-stage increase in white matter anisotropy takes place at different rates for different brain areas, as does brain maturation(21).

Regional anisotropy is clearly influenced by other factors than myelination alone, such as axon packing, relative membrane permeability to water, internal axonal structure, and tissue water content.

Another brain area in which anisotropy values differ between immature and mature brain is cerebral cortex. Anisotropy values of cortical grey matter in adult brain are generally consistent with zero (*i.e.*, diffusion is isotropic). As shown in several human and animal studies now, values for cortical grey matter in immature brain are transiently nonzero during development (22-25). A recent study on human fetal brain has shown that cortical anisotropy increases from 15 weeks gestation to approx. 27 weeks gestation and then shows a gradual decline to 32 weeks gestation (26). The increase of anisotropy in this time period coincides with active neuronal migration along the radial glial scaffolding, whereas the decrease coincides with the phase of neocortical maturation with transformation of the radial glia into the more complex astrocytic neuropil. During the gestational ages for which anisotropy values are nonzero, cortical cytoarchitecture is therefore dominated by the radial glial fibers that are present across the cortical strata and by the radially-oriented apical dendrites of pyramidal cells(27). With time, this architecture is disrupted by the addition of basal dendrites as well as thalamocortical afferents, which tend to be oriented orthogonal to the apical dendrites. Again these observation of microstructural brain development are not homogenous throughout the brain but show considerable regional differences, with cortical anisotropy decreasing first in precentral cortex, followed by occipital and frontal cortex (28) and even changing laterality throughout development(26). Unlike the changes observed in immature white matter the change in fractional anisotropy observed in the cortex are mainly due to significant decrease in  $\lambda_1$  with no changes in  $\lambda_2$  and  $\lambda_3$  (28). Thus, the relatively large decline in  $\lambda_1$ , oriented radially in 25 to 40 weeks gestation cortex means that the maturational loss of cortical anisotropy is due to a reduction in the radial component of water diffusivity. Thus developmental changes in anisotropy of cerebral cortex reflect changes in its microstructure, such as the arborization of basal dendrites of cortical neurons, the innervation of the cortical plate by thalamocortical and cortico-cortical fibers, transformation of radial glia into mature astrocytes, all processes, which are an important basis of later functional connectivity.

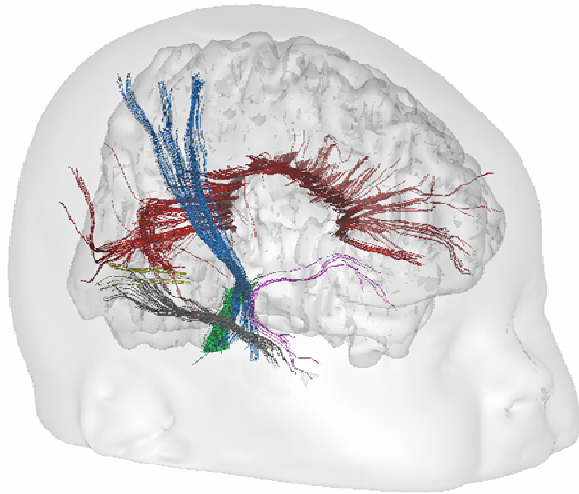
Vector maps also provide information regarding anisotropy. In the case of cortical grey matter, the vectors are oriented radially, consistent with the orientation of the radial glial fibers and apical dendrites of pyramidal cells (22). Vector maps of white matter provide a visual indication of white matter organization. Thus it is possible to produce an image of the overall orientation of white matter fibers in a given area.

The very immature brain is further characterized by a laminar organization with an immature cortical plate (as described above), a prominent subplate, an intermediate zone (corresponding to the later white matter) and the important area of germinal matrix, the origin of both neuronal and glial cell migration. Using vector maps derived from DTI this laminar organization can be visualized both in the immature primate (25) as well as human brain (23). Using an advanced pixel classification system in which specific patterns of  $D_{av}$  and anisotropy are detected automatically the immature human brain can be subdivided into cortical plate, subplate zone, deep-to subplate layers including the intermediate zone the subventricular zone and the germinal matrix(23). The germinal matrix itself was shown to express a gestational dependent decrease in

anisotropy from 15 weeks gestation to about 32 weeks, when the germinal matrix starts to disappear (26).

Fiber tracking is another recent technique applied to the developing brain to study quantitative assessment of specific pathway maturation (29)

Figure 2. Major white matter fiber tracts in a term newborn (30).



course through the brain (32).

Bermann et al (31) were able to show significant differences in the maturational changes in fractional anisotropy and transverse diffusion between the motor and the somatosensory pathway in premature infants between 30 and 40 weeks gestational age. This approach further allowed to measure diffusion changes across multiple levels of the functional tract (31).

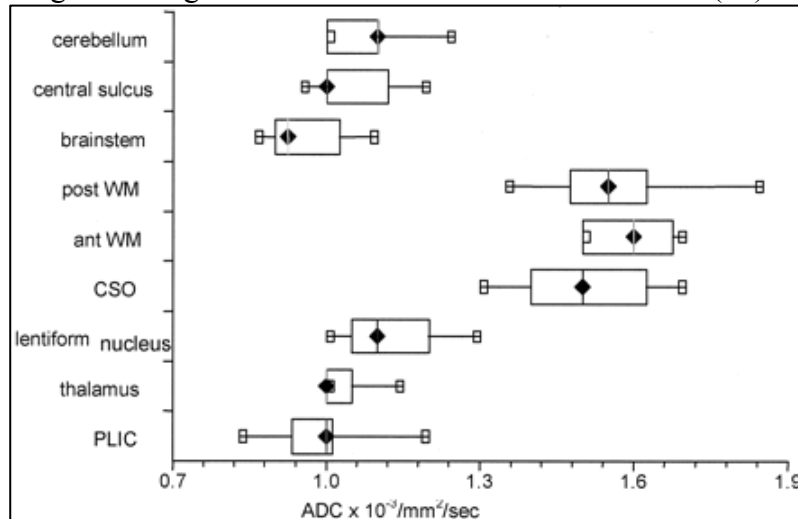
Alteration of white matter organisation in preterm infants compared to fullterm newborns have been shown using DTI (12). As discussed below, this orientation may be disrupted due to injury. It is also worth noting that vector maps can be used to follow white matter tracts as they

### **DTI and Injury during brain development**

Neonatal brain injury is either characterized by hypoperfusion and/or hypoxemia followed by reperfusion as the infant is resuscitated, typically shortly after delivery or by chronic exposure to infection and inflammation. Hypotheses put forth to explain brain injury often take both mechanisms – hypoxia/ischemia and reperfusion and infection/inflammation – into account. Neuronal death appears to involve both necrosis and apoptosis (33). Molecular mechanisms proposed to explain injury to both neurons and glia include accumulation of: cytosolic calcium, free radicals (including nitric oxide), cytotoxic amino acids, and cytokines (34). Periventricular leukomalacia, PVL, is a unique pattern of neonatal brain injury that is most often found in preterm infants. Pathologic abnormalities are characteristically localized to the white matter dorsal and lateral to the external angles of the lateral ventricles and involve primarily the centrum semiovale (35). This white matter region is thought especially vulnerable to injury in the preterm infant because of the nature of its blood supply and particular sensitivity to proinflammatory cytokines triggered by stimuli such as hypoxia-ischemia and infection (36).

As indicated in the introduction, values for  $D_{av}$  decrease quickly after injury in most models studied, providing evidence of injury on maps of  $D_{av}$  before the injury is detectable on conventional imaging. The decrease in water diffusion associated with injury was initially described for animal(37, 38) and adult human (4) stroke, and was subsequently confirmed for human infants (39). Interpretation of ADC values to detect acute brain injury in the developing brain needs to be adjusted for the regional differences in ADC values according to age.

Figure 3: Regional ADC values in the newborn brain (39)



There is not yet a consensus on the precise mechanism for the decrease in  $D_{av}$  associated with injury. Changes in  $D_{av}$  following injury are dynamic.  $D_{av}$  values are initially decreased, but subsequently increase so that they are greater than normal and remain so in the chronic phase of injury. During the transition between decreased and increased values there is a brief period during which values are normal, a process referred to as «pseudonormalization.» Pseudonormalization takes place roughly two days following stroke in a rat model (40) and at approximately nine days following injury in adult human stroke (41). Preliminary data indicate that the timing of pseudonormalization in human newborns more closely follows that of adult humans than rodents, taking place at roughly seven days following the injury (42). The time course of these changes is complex, however, and may vary somewhat with the nature of the injury (hypoxia-ischemia, inflammation, trauma), the relative vulnerability of different brain areas to injury, and other processes such as primary and secondary energy failure (43). Given the dynamic nature of these changes, it has been suggested that a combination of conventional and DTI images and magnetic resonance spectroscopy can be used to estimate the age of an injury to the central nervous system. During the first days following an injury, there are abnormalities on  $D_{av}$  maps, due to decreased water  $D_{av}$ , but not T2-weighted images. Subsequently, abnormalities are visible on both  $D_{av}$  maps and T2-weighted images. Roughly one week after the injury, the  $D_{av}$  map will become normal due to pseudonormalization, but the injury will be visible on T2-weighted images. With chronic injury, the lesion will be visible again on  $D_{av}$  maps, but now as an increase in water  $D_{av}$  rather than a decrease (44).

The dynamic nature of the changes in  $D_{av}$  following injury makes it difficult to directly compare conventional MRI with DTI for detection of injury. Which method is most sensitive to injury – T2-weighted imaging, T1-weighted imaging, or  $D_{av}$  maps – varies with time after injury. Studies in which MR imaging is done at roughly one week after injury, the approximate time at which pseudonormalization takes place, tend to find that conventional imaging is as good as or better than DTI(45). Studies in which the imaging is done somewhat earlier tend to find more utility for DTI(46). Studies in which a series of images are obtained from the same infant over time(42) indicate that DTI is more useful during the first few days after injury, whereas conventional imaging, particularly T2-weighted or FLAIR imaging, is more useful at later times. Overall, the primary difference between DTI and conventional imaging is the capability of DTI to often detect injury earlier. This may offer advantages in the future if neuroprotective agents

become available and early detection of injury becomes important for deciding whether or not to administer them to a particular patient. It is worth noting, however, that DTI may not necessarily always demonstrate injury earlier than conventional MR imaging and MRS might indicate metabolic alterations in otherwise normal imaging studies prior to 24h after injury(42, 47-49).

Anisotropy of white matter also changes following injury. The changes appear to take place over several days to weeks. At the simplest level, anisotropy values are reduced dramatically in areas in which white matter is lost, such as porencephalic cysts(50). Studies with pediatric and neonatal stroke also indicate that Wallerian degeneration is detectable as changes in anisotropy distant from the site of infarction (51). Changes in anisotropy involving both anisotropy measurements and vector maps will likely prove especially relevant in premature infants, who tend to sustain injury to white matter. In the chronic stage of PVL, reductions in relative anisotropy may be present and vector maps may show disruption of white matter tracts distant from the focal, cystic lesions detected by conventional imaging (52). In this case, changes in anisotropy are detectable not only near the site of primary injury (the periventricular white matter), but also in the posterior limb of the internal capsule, indicating a disturbance of developing fibers which project through this area (52). Thus, anisotropy and vector maps demonstrate injury that is not detectable by more conventional means. Further, changes in RA and fiber maps may provide insight into post-injury brain plasticity (53, 54). The clinical relevance of injury and related modification of white matter architecture detected in this fashion is not yet known, and long-term follow up studies are currently underway (55).

### **Conclusions**

Important changes in water apparent diffusion coefficient and diffusion anisotropy accompany brain maturation. These changes reflect changes in brain tissue microstructure. In the case of grey matter, this may reflect changes in the dendritic architecture of pyramidal cells, the presence or absence of radial glial fibers. In the case of white matter, this is due to both «premyelination» changes and myelination itself. Thus DTI offers a unique, noninvasive window into brain maturation which can be readily applied to human development.

DTI parameters also show distinct changes in response to brain injury. Decreases in the water apparent diffusion coefficient may serve as an early indicator of brain injury which could prove useful in the context of rapidly determining the presence/absence of injury in anticipation of therapeutic intervention with neuroprotective therapies for the developing brain. Chronic changes in water anisotropy and the evaluation by DTI vector imaging are sensitive to injury-related impairment of subsequent white matter development and brain connectivity, providing evidence of disruption in areas much more widespread than detected through conventional imaging. Thus DTI is potentially of great value clinically for evaluation of injury and plasticity in developing brain.

### **Reference List**

1. Basser P, Pierpaoli C 1996 Microstructural and physiological features of tissues elucidated by

quantitative-diffusion-tensor MRI. *J Magn Reson B* 11:209-219

2. Neil J, Miller J, Mukherjee P, Huppi PS 2002 Diffusion tensor imaging of normal and injured developing human brain - a technical review. *NMR Biomed* 15:543-552
3. Rumpel H, Nedelcu J, Aguzzi A, Martin E 1997 Late glial swelling after acute cerebral hypoxia-ischemia in the neonatal rat: A combined magnetic resonance and histochemical study. *Pediatr Res* 42:54-59
4. Warach S, Chien D, Li W 1992 Fast magnetic resonance diffusion-weighted imaging of acute human stroke. *Neurology* 42:1717-1723
5. Rutherford MA, Azzopardi D, Whitelaw A, Cowan F, Renowden S, Edwards AD, Thoresen M 2005 Mild hypothermia and the distribution of cerebral lesions in neonates with hypoxic-ischemic encephalopathy. *Pediatrics* 116:1001-1006
6. Inder T, Huppi P, Zientara G, Maier S, Jolesz F, di Salvo D, Robertson R, Barnes P, Volpe J 1999 Early detection of periventricular leukomalacia by diffusion-weighted magnetic resonance imaging techniques. *J Pediatr* 134:631-634
7. Glenn OA, Henry RG, Berman JI, Chang PC, Miller SP, Vigneron DB, Barkovich AJ 2003 DTI-based three-dimensional tractography detects differences in the pyramidal tracts of infants and children with congenital hemiparesis  
*J Magn Reson Imaging* 18:641-648
8. Mori S, van Zijl PC 1995 Diffusion weighting by the trace of the diffusion tensor within a single scan. *Magn Reson Med* 33:41-52
9. Ulug AM, van Zijl PC 1999 Orientation-independent diffusion imaging without tensor diagonalization: anisotropy definitions based on physical attributes of the diffusion ellipsoid. *J Magn Reson Imaging* 9:804-813
10. Hasan KM, Alexander AL, Narayana PA 2004 Does fractional anisotropy have better noise immunity characteristics than relative anisotropy in diffusion tensor MRI? An analytical approach. *Magn Reson Med* 51:413-417
11. Conturo TE, McKinstry RC, Aronovitz JA, Neil JJ 1995 Diffusion MRI: precision, accuracy and flow effects. *NMR Biomed* 8:307-332
12. Hüppi P, Maier S, Peled S, Zientara G, Barnes P, Jolesz F, Volpe J 1998 Microstructural development of human newborns cerebral white matter assessed in vivo by diffusion tensor MRI. *Pediatr Res* 44:584-590
13. Neil J, Shiran S, McKinstry R, Schefft G, Snyder A, Almlı C, Akbudak E, Aronovitz J, Miller J, Lee B, Conturo T 1998 Normal brain in human newborns: Apparent diffusion coefficient and diffusion anisotropy measured by using diffusion tensor MR Imaging. *Radiology* 209:57-66
14. Mukherjee P, Miller JH, Shimony JS, Philip JV, Nehra D, Snyder AZ, Conturo TE, Neil JJ, McKinstry RC 2002 Diffusion-tensor MR imaging of gray and white matter development during normal human brain maturation. *AJNR Am J Neuroradiol* 23:1445-1456

15. Boujraf S, Luypaert R, Shabana W, De Meirleir L, Sourbron S, Osteaux M 2002 Study of pediatric brain development using magnetic resonance imaging of anisotropic diffusion. *Magn Reson Imaging* 20:327-336
16. Partridge SC, Mukherjee P, Henry RG, Miller SP, Berman JI, Jin H, Lu Y, Glenn OA, Ferriero DM, Barkovich AJ, Vigneron DB 2004 Diffusion tensor imaging: serial quantitation of white matter tract maturity in premature newborns. *Neuroimage* 22:1302-1314
17. Ulug AM, Beauchamp N, Jr., Bryan RN, van Zijl PC 1997 Absolute quantitation of diffusion constants in human stroke. *Stroke* 28:483-490
18. Klingberg T, Vaidya CJ, Gabrieli JD, Moseley ME, Hedehus M 1999 Myelination and organization of the frontal white matter in children: a diffusion tensor MRI study. *Neuroreport* 10:2817-2821
19. Wimberger DM, Roberts TP, Barkovich AJ, Prayer LM, Moseley ME, Kucharczyk J 1995 Identification of "premyelination" by diffusion-weighted MRI. *J Computr Assisted Tomography* 19:28-33
20. Kinney H, Brody B, Kloman A, Gilles F 1988 Sequence of central nervous system myelination in human infancy. II Patterns of myelination in autopsied infants. *J Neuropathol Exp Neurol* 47(3):217-234
21. Brody B, Kinney H, Kloman A, Gilles F 1987 Sequence of central nervous system myelination in human infancy. I An autopsy study of myelination. *J Neuropathol Exp Neurol* 46(3):283-301
22. McKinstry RC, Mathur A, Miller JH, Ozcan A, Snyder AZ, Schefft GL, Almlri CR, Shiran SI, Conturo TE, Neil JJ 2002 Radial organization of developing preterm human cerebral cortex revealed by non-invasive water diffusion anisotropy MRI. *Cereb Cortex* 12:1237-1243
23. Maas LC, Mukherjee P, Carballido-Gamio J, Veeraraghavan S, Miller SP, Partridge SC, Henry RG, Barkovich AJ, Vigneron DB 2004 Early laminar organization of the human cerebrum demonstrated with diffusion tensor imaging in extremely premature infants. *Neuroimage* 22:1134-1140
24. Mori S, Itoh R, Zhang J, Kaufmann WE, van Zijl PC, Solaiyappan M, Yarowsky P 2001 Diffusion tensor imaging of the developing mouse brain. *Magn Reson Med* 46:18-23
25. Kroenke CD, Bretthorst GL, Inder TE, Neil JJ 2005 Diffusion MR imaging characteristics of the developing primate brain. *Neuroimage* 25:1205-1213
26. Gupta RK, Hasan KM, Trivedi R, Pradhan M, Das V, Parikh NA, Narayana PA 2005 Diffusion tensor imaging of the developing human cerebrum. *J Neurosci Res* 81:172-178
27. Marin-Padilla M 1992 Ontogenesis of the pyramidal cell of the mammalian neocortex and developmental cytoarchitectonics: a unifying theory. *J Comp Neurol* 321:223-240
28. Deipolyi AR, Mukherjee P, Gill K, Henry RG, Partridge SC, Veeraraghavan S, Jin H, Lu Y, Miller SP, Ferriero DM, Vigneron DB, Barkovich AJ 2005 Comparing microstructural and macrostructural development of the cerebral cortex in premature newborns: diffusion tensor imaging versus cortical gyration. *Neuroimage* 27:579-586

29. Watts R, Liston C, Niogi S, Ulug AM 2003 Fiber tracking using magnetic resonance diffusion tensor imaging and its applications to human brain development. *Ment Retard Dev Disabil Res Rev* 9:168-177
30. Dubois J, Hertz-Pannier, L., Dehaene-Lambert G, Cointepas, Y., and Le Bihan D. Assessment of the early organisation and maturation of infants cerebral white matter fiber bundles: a feasibility study using quantitative diffusion tensor imaging and tractography. *Neuroimage*. 2005. In Press
31. Berman JI, Mukherjee P, Partridge SC, Miller SP, Ferriero DM, Barkovich AJ, Vigneron DB, Henry RG 2005 Quantitative diffusion tensor MRI fiber tractography of sensorimotor white matter development in premature infants. *Neuroimage* 27:862-871
32. Mamata H, Mamata Y, Westin CF, Shenton ME, Kikinis R, Jolesz FA, Maier SE 2002 High-resolution line scan diffusion tensor MR imaging of white matter fiber tract anatomy. *AJNR Am J Neuroradiol* 23:67-75
33. Edwards AD, Yue X, Squier MV, Thoresen M, Cady EB, Penrice J, Cooper CE, Wyatt JS, Reynolds EO, Mehmet H 1995 Specific inhibition of apoptosis after cerebral hypoxia-ischaemia by moderate post-insult hypothermia. *Biochem Biophys Res Commun* 217:1193-1199
34. Huppi PS 2002 Advances in postnatal neuroimaging: relevance to pathogenesis and treatment of brain injury. *Clin Perinatol* 29:827-856
35. Banker B, Larroche J 1962 Periventricular leukomalacia of infancy. *Arch Neurol* 7:386-410
36. Dammann O, Kuban KC, Leviton A 2002 Perinatal infection, fetal inflammatory response, white matter damage, and cognitive limitations in children born preterm *Ment Retard Dev Disabil Res Rev* 8:46-50
37. Moseley M, Cohen Y, Kucharczyk J, Mintorovitch J, Asgari H, Wendland M, Tsuruda J, Norman D 1990 Diffusion-weighted MR-imaging of anisotropic water diffusion in cat central nervous system. *Radiology* 176:439-445
38. Rumpel H, Ferrini B, Martin E 1998 Lasting cytotoxic edema as an indicator of irreversible brain damage: A case of neonatal stroke. *Neurosci Behav* 19:1636-1638
39. Rutherford M, Counsell S, Allsop J, Boardman J, Kapellou O, Larkman D, Hajnal J, Edwards D, Cowan F 2004 Diffusion-weighted magnetic resonance imaging in term perinatal brain injury: a comparison with site of lesion and time from birth. *Pediatrics* 114:1004-1014
40. Li F, Han SS, Tatlisumak T, Liu KF, Garcia JH, Sotak CH, Fisher M 1999 Reversal of acute apparent diffusion coefficient abnormalities and delayed neuronal death following transient focal cerebral ischemia in rats. *Ann Neurol* 46:333-342
41. Copen WA, Schwamm LH, Gonzalez RG, Wu O, Harmath CB, Schaefer PW, Koroshetz WJ, Sorensen AG 2001 Ischemic stroke: effects of etiology and patient age on the time course of the core apparent diffusion coefficient. *Radiology* 221:27-34
42. McKinstry RC, Miller JH, Snyder AZ, Mathur A, Schefft GL, Almli CR, Shimony JS, Shiran SI,

Neil JJ 2002 A prospective, longitudinal diffusion tensor imaging study of brain injury in newborns. *Neurology* 59:824-833

43. Li F, Liu KF, Silva MD, Meng X, Gerriets T, Helmer KG, Fenstermacher JD, Sotak CH, Fisher M 2002 Acute postischemic renormalization of the apparent diffusion coefficient of water is not associated with reversal of astrocytic swelling and neuronal shrinkage in rats. *AJNR Am J Neuroradiol* 23:180-188
44. Counsell SJ, Allsop JM, Harrison MC, Larkman DJ, Kennea NL, Kapellou O, Cowan FM, Hajnal JV, Edwards AD, Rutherford MA 2003 Diffusion-weighted imaging of the brain in preterm infants with focal and diffuse white matter abnormality  
*Pediatrics* 112:1-7
45. Welch KM, Windham J, Knight RA, Nagesh V, Hugg JW, Jacobs M, Peck D, Booker P, Dereski MO, Levine SR 1995 A model to predict the histopathology of human stroke using diffusion and T2-weighted magnetic resonance imaging. *Stroke* 26:1983-1989
46. Wolf R, Zimmerman R, Clancy R, Haselgrove J 2001 Quantitative apparent diffusion coefficient measurements in term neonates for early detection of hypoxic-ischemic brain injury: initial experience. *Radiology* 218:825-833
47. Soul JS, Robertson RL, Tzika AA, du Plessis AJ, Volpe JJ 2001 Time course of changes in diffusion-weighted magnetic resonance imaging in a case of neonatal encephalopathy with defined onset and duration of hypoxic-ischemic insult. *Pediatrics* 108:1211-1214
48. Zarifi MK, Astrakas LG, Poussaint TY, Plessis AA, Zurakowski D, Tzika AA 2002 Prediction of adverse outcome with cerebral lactate level and apparent diffusion coefficient in infants with perinatal asphyxia. *Radiology* 225:859-870
49. L'abee C, de Vries LS, van Der GJ, Groenendaal F 2005 Early Diffusion-Weighted MRI and H-Magnetic Resonance Spectroscopy in Asphyxiated Full-Term Neonates. *Biol Neonate* 88:306-312
50. Pierpaoli C, Barnett A, Pajevic S, Chen R, Penix LR, Virta A, Basser P 2001 Water diffusion changes in Wallerian degeneration and their dependence on white matter architecture. *Neuroimage* 13:1174-1185
51. de Vries LS, van Der GJ, van Haastert IC, Groenendaal F 2005 Prediction of outcome in new-born infants with arterial ischaemic stroke using diffusion-weighted magnetic resonance imaging. *Neuropediatrics* 36:12-20
52. Hüppi P, Murphy B, Maier S, Zientara G, Inder T, Barnes P, Kikinis R, Jolesz F, Volpe J 2001 Microstructural brain development after perinatal cerebral white matter injury assessed by diffusion tensor magnetic resonance imaging. *Pediatrics* 107:455-460
53. Nagy Z, Westerberg H, Skare S, Andersson JL, Lilja A, Flodmark O, Fernell E, Holmberg K, Bohm B, Forssberg H, Lagercrantz H, Klingberg T 2003 Preterm children have disturbances of white matter at 11 years of age as shown by diffusion tensor imaging  
*Pediatr Res* 54:672-679
54. Thomas B, Eyssen M, Peeters R, Molenaers G, Van Hecke P, De Cock P, Sunaert S 2005

Quantitative diffusion tensor imaging in cerebral palsy due to periventricular white matter injury.  
Brain 128:2562-2577

55. Olesen PJ, Nagy Z, Westerberg H, Klingberg T 2003 Combined analysis of DTI and fMRI data reveals a joint maturation of white and grey matter in a fronto-parietal network  
Brain Res Cogn Brain Res 18:48-57